This is a repository copy of *Discovery and Optimization of wt-RET/KDR-Selective Inhibitors of RETV804M Kinase*.

White Rose Research Online URL for this paper:
http://eprints.whiterose.ac.uk/159089/

Version: Accepted Version

Discovery and Optimisation of wt-RET/KDR-selective Inhibitors of RET^{V804M} Kinase

Rebecca Newton,[1,*] Bohdan Waszkowycz,[1] Chitra Seewooruthun,[2] Daniel Burschowsky,[2] Mark Richards,[3] Samantha Hitchin,[1] Habiba Begum,[1] Amanda Watson[1], Eleanor French,[1] Niall Hamilton,[1] Stuart Jones,[1] Li-Ying Lin,[4] Ian Waddell,[1] Aude Echalier,[2] Richard Bayliss,[3] Allan M. Jordan[1] and Donald Ogilvie.[1]

[1]*Drug Discovery Unit, Cancer Research UK Manchester Institute University of Manchester, Alderley Park, Macclesfield, SK10 4TG. U.K.*

[2]*Department of Molecular and Cell Biology, Henry Wellcome Building, University of Leicester, Lancaster Road, Leicester, LE1 7RH, UK.*

[3]*Astbury Centre for Structural Molecular Biology, Faculty of Biological Sciences, University of Leeds, Leeds, LS2 9JT, UK.*

[4]*Leicester Drug Discovery & Diagnostics Centre (LD3), R407a, Hodgkin Building, Lancaster Road, Leicester, LE1 7HB, UK.*

ABSTRACT

A combination of focussed library and virtual screening, hit expansion and rational design has resulted in the development of a series of inhibitors of RET^{V804M} kinase, the anticipated drug-resistant mutant of RET kinase. These agents do not inhibit the wild type (wt) isoforms of RET or KDR and therefore offer a potential adjunct to RET inhibitors currently undergoing clinical evaluation.

Keywords: RET, KDR, kinase inhibitor, virtual screening

Activating gene fusions of the receptor tyrosine kinase RET have recently been identified as drivers in around 1-2% of all non-small cell lung cancers (NSCLC).[1-3] In non-smokers, the incidence of these mutations rises to around 6%.[4] Following the clinical success of similar agents targeting other lung cancer driver mutations, such as EGFR and ALK, there has been a recent resurgence of interest in developing inhibitors of the RET kinase domain.

Whilst the clinically approved agents vandetanib **1** and cabozantinib **2** are being extensively evaluated in clinical trials for this indication, RET inhibition is a secondary pharmacology of these compounds. The primary pharmacology of these agents, namely inhibition of KDR (or VEGFR2), leads to dose-limiting side effects, significantly compromising their therapeutic utility in NSCLC.[5,6] Given this observed clinical toxicity, more selective RET inhibitors, devoid of

KDR inhibitory activity *in vivo*, have been of considerable interest and agents such as LOXO-292 **3** and BLU-667 **4** are now being evaluated in clinical trials (Figure 1).[7,8]
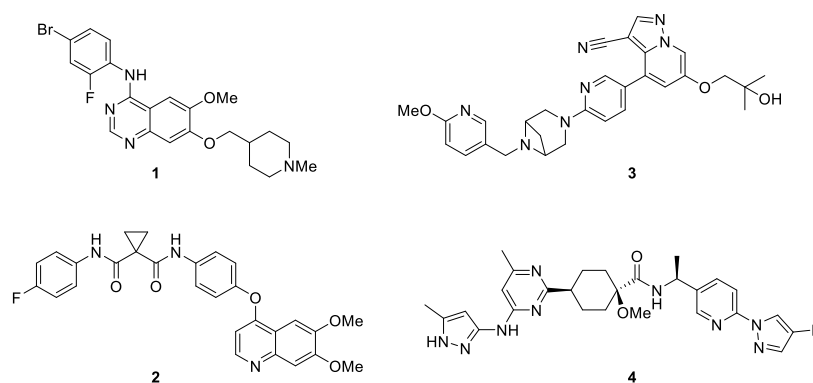

Figure 1: *Exemplar first generation non-selective and second generation (KDR-selective) RET inhibitors.*

However, patients treated with kinase inhibitors are frequently prone to early clinical relapse due to mutations in the kinase ATP binding domain, which render the protein catalytically active but no longer sensitive to drug treatment. Such mutations often occur in the so-called "gatekeeper" region. In the case of RET, resistance is predicted to arise from a Val to Met or Leu mutation at residue 804.[9] Anticipating this outcome, second generation RET-selective inhibitors **3** and **4** also inhibit the gatekeeper mutant (RET$^{V804M/L}$) kinase domain.[7,8]

At the outset of this study, clinical data for selective RET inhibitors was unavailable, and as such the dose-limiting toxicity of a truly RET-selective inhibitor was unknown. Drawing on the precedent of inhibitors of EGFR in lung cancer, where wild type-sparing mtEGFR inhibitors offer significant clinical advantage,[10] we hypothesised that a RET$^{V804M/L}$-selective, rather than mixed wild type/gatekeeper mutant inhibitor, may offer an alternate therapeutic option for patients with refractory disease, particularly if robust RET inhibition was shown to induce significant tolerability issues. Such an agent would allow more robust inhibition of the target and may deliver enhanced therapeutic benefit. Further, a RET^{V804M} selective agent may serve as a useful adjunct therapy alongside RET-selective agents, which do not maintain activity against the anticipated gatekeeper resistance mutants.[11]

To deliver RET^{V804M}-selective inhibitors, we decided to implement screening of a commercial kinase-directed library of just over nine thousand compounds, alongside a virtual screening cascade based on docking to in-house RET^{V804M} homology models, derived in turn from published wild type RET kinase domain crystal structures (PDB 2IVU and 2IVT). We reasoned that the mutated gatekeeper sidechain, replacing a small Val by a larger Met/Leu, occludes access to the hydrophobic pocket normally exploited by compounds such as **1**, hence their loss of binding affinity for RET^{V804M}.[12] We therefore sought to identify ligands that avoided this pocket and bound primarily to the site otherwise

occupied by ATP. Whilst such ligands retain the potential to inhibit RET, our intention was primarily to identify ligands that would not be penalised by the mutation, though we recognised that there was a risk of reducing selectivity over other kinases, as the hydrophobic pocket contributes to the kinome selectivity profile of compounds such as **1**. However, we postulated that the desired selectivity over RET might then arise by virtue of enhanced contacts between the ligand and the more hydrophobic mutated gatekeeper, or (more serendipitously) by a particular scaffold potentially exploiting other more subtle structural differences between the two binding sites.

To this end, a library of 984,000 lead-like compounds (internally triaged from the eMolecules screening collection[13]) was docked against our homology models (Glide HTVS and SP docking, Schrödinger, LLC, New York) and manual triage of the resultant hits undertaken, with selection based upon factors including docking score, maintenance of the key hinge-binding interactions, clustering by 2D chemotype and visual assessment of binding poses, assessing both novelty of interactions and potential for selectivity against RET and KDR. From this exercise, we selected a set of 197 compounds, for purchase and screening in biochemical assays against our three key targets. Pleasingly, several of these early derivatives were found to show promising selectivity of up to 100-fold against both RET and KDR (Figure 2a) and these clustered predominantly into five distinct chemotypes. These encouraging start-points (four clusters derived from virtual screening and one from the kinase-focussed library) were further elaborated through both analogue-by-catalogue hit expansion and modelling-directed analogue synthesis, rapidly delivering both increased potency and selectivity against key off-targets across several series (Figure 2b).
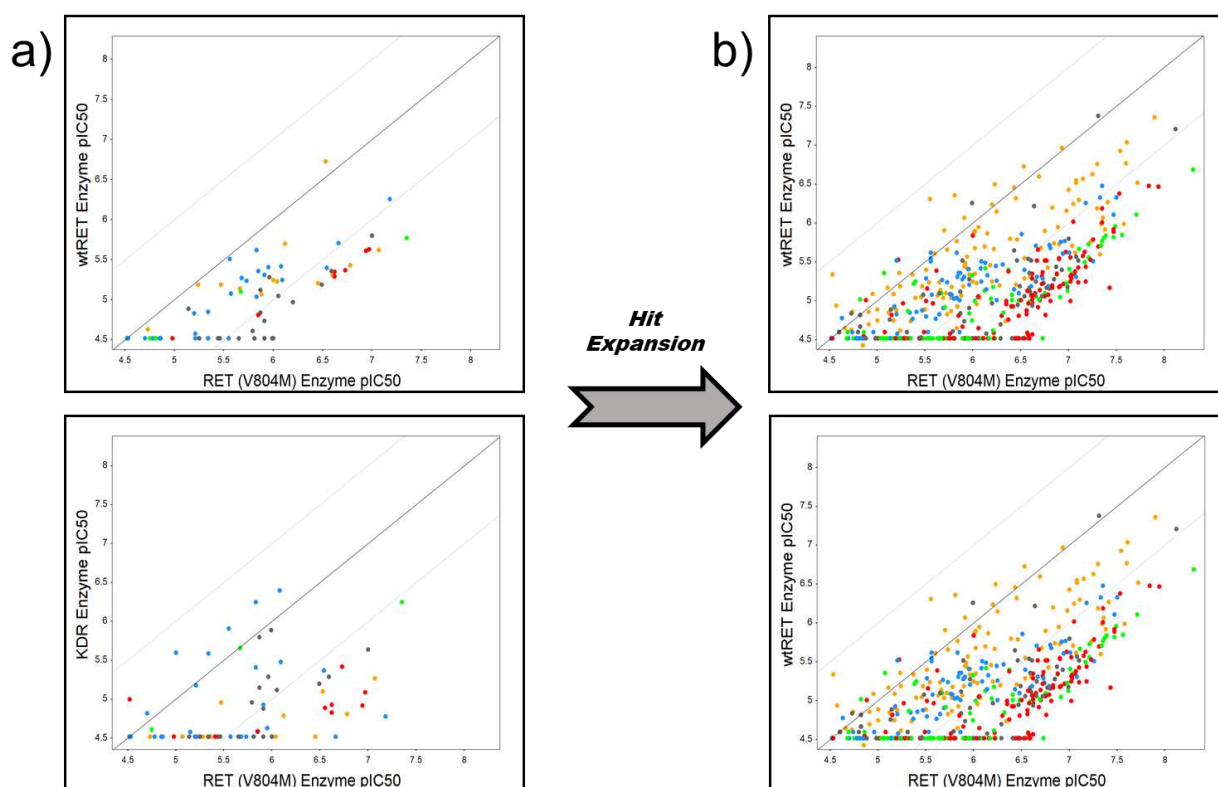
Figure 2: *a) Selectivity profile of hits obtained from initial kinase library and virtual screen; b) Hit expansion through analogue by catalogue and focussed synthesis. In both cases, plots display RET^{V804M} biochemical pIC_{50} vs wt-RET pIC_{50} (upper panel) and KDR pIC_{50} (lower panel). Colours indicate the five identified chemotypes of interest. Desirable hits are found in the lower right quadrant of each plot.*

From these early studies, we became particularly interested in hits derived from a pyrazolopyrimidine scaffold (Figure 2, orange dots), exemplified by the benzamide analogue **5** (Figure 3). Whilst related pyrazolo[3,4-d]pyrimidin-4-amines have been described previously by Yoon[14] and others,[15,16] these derivatives have been generally shown to be more potent inhibitors of wild type RET than RET^{V804M}. This observation perhaps makes the initial selectivity profile observed with this early pyrazolo[1,5-a]pyrimidin-5-amine all the more surprising. Docking of compound **5** (Figure 4a) suggested an attractive binding mode with options to enhance both RET and KDR selectivity. We predicted that the pyrazolopyrimidine core would bind to the hinge region, directing the benzamide towards the catalytic lysine (Lys758) and placing the pyridine in the pocket normally occupied by the ribose moiety of ATP. Both of these sites offer opportunities for optimising protein-ligand interactions to improve affinity and selectivity; for example, the ribose pocket is bounded by residues Ser811 and Ser891 which are not conserved between RET and KDR. Our interest was further enhanced after biochemical evaluation, which demonstrated the compound to be over 100-fold selective against KDR and almost 4-fold selective against RET. The compound also demonstrated modest cellular potency against our RET^{V804M} cell assay, albeit with a considerable decrease in selectivity.
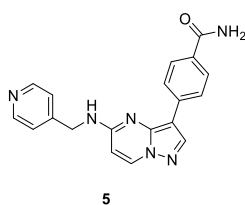

Figure 3: *Early pyrazolopyrimidine hit **5**.*

To permit exploration of structure-activity relationships, analogues of **5** were prepared from commercially available pyrazolopyrimidine **6**, through S_NAr displacement to give intermediates **7-10** and Pd-mediated coupling, as described in Scheme 1. **1** and **2** were used as benchmark compounds for our subsequent studies. As shown in Table 1, both were more active against wild type RET and KDR than they were against RET^{V804M}. Early structure-activity relationship investigations suggested that the amide motif of **5** was important for binding, with the dimethyl derivative **11** showing a significant loss of activity in our biochemical assay (Table 1). The regiochemistry of the pendant pyridyl moiety was also investigated (compounds **12** and **13**), though the position of the nitrogen did not result in any significant alteration

to potency or selectivity, suggesting that the nitrogen atom itself does not participate in a specific, directional hydrogen-bonding interaction. However, the simple incorporation of a basic nitrogen in a similar spatial region (compound **14**) resulted in a ten-fold reduction in potency.

Scheme 1: *Synthesis of compounds* ***5, 11-23.***
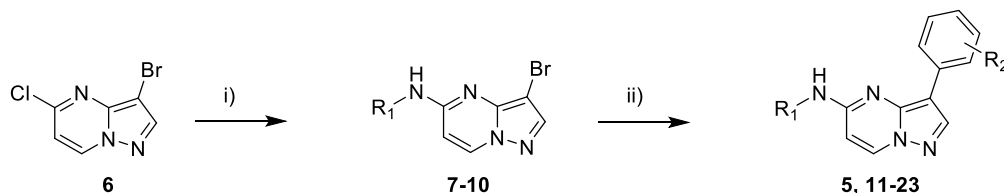
Reagents and conditions: i) R_1-NH$_2$, DIPEA, IPA, 100 °C, 5h, 47-100%; ii) arylboronic acid, K_3PO_4, Pd-118, 1,4-dioxane, water, μwave, 120 °C, 30 min, 7-34%

Further studies confirmed that removal of the amide functionality (compound **15**) resulted in a significant loss of biochemical potency as did movement of the amide from the *para-* to *meta-*position (compound **16**) (Table 2). The corresponding sulphonamide **17** and carboxylic acid **18** were reasonably well tolerated. Reversal of the amide or sulphonamide (compounds **19-21**) was detrimental to potency. These results were generally consistent with our hypothesised binding mode, suggesting that specific H-bonding interactions between the benzamide of **5** and Lys758 were important for potency. Further exploration of the SAR around this ring gave disappointing results (data not shown), but led to the suggestion to mimic the primary amide in a bicyclic system. These investigations led to **22** and, whilst this compound was ten-fold less potent than **5** in biochemical assays, RET selectivity was improved considerably. Of more interest, **5** and **22** were roughly equipotent in our RET[V804M] cell assay, despite the differences in biochemical activity. Whilst this cellular selectivity was only a modest two-fold at this stage, we felt that this derivative offered potential for further gains and a wider exploration of bicyclic systems was undertaken, leading to **23**. Whilst this compound appeared less impressive in terms of selectivity in our biochemical assays than **22**, it did display moderately improved cell potency and slightly improved cell selectivity against both the RET and KDR driven cell lines.

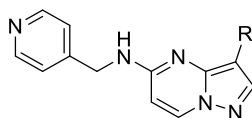*Table 1: Initial optimisation of hit pyrazolopyrimidine **5**.[a]*
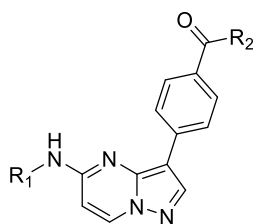
Compound	R1	R2	RET^{V804M} biochemical IC$_{50}$ (μM)	Biochemical selectivity, RET^{V804M} vs RET	Biochemical selectivity, RET^{V804M} vs KDR	RET^{V804M} cellular IC$_{50}$ (μM)	Cell assay selectivity, RET^{V804M} vs RET	Cell assay selectivity, RET^{V804M} vs KDR
1	-	-	>5	0.009	0.03	1.5 (0.92)	0.24	0.43
2	-	-	1.5 (2.4)	0.33	0.01	0.18 (0.069)	1.1	0.08
5	pyridin-4-ylethyl	NH$_2$	0.02 (0.007)	3.7	110	4.4 (0.18)	0.89	2.3
11	pyridin-4-ylethyl	NMe$_2$	7.6 (1.0)	1.8	3.9			
12	pyridin-2-ylethyl	NH$_2$	0.044 (0.014)	19	22	3.7 (0.41)	0.90	2.0
13	pyridin-3-ylethyl	NH$_2$	0.051 (0.0078)	13	19	3.9 (0.20)	0.85	1.9
14	dimethylaminoethyl	NH$_2$	0.35 (0.034)	4.7	54	> 10	0.30	0.83

[a]*All assay values are the geometric mean of at least two independent duplicate determinations, quoted to two significant figures.*

Standard deviations are given in parentheses. Biochemical and cellular selectivities are expressed as fold-values.

*Table 2: Further optimisation of hit pyrazolopyrimidine 5.[a]*

Compound	R	RET^{V804M} biochemical IC$_{50}$ (µM)	Biochemical selectivity, RET^{V804M} vs RET	Biochemical selectivity, RET^{V804M} vs KDR	RET^{V804M} cellular IC$_{50}$ (µM)	Cell assay selectivity, RET^{V804M} vs RET	Cell assay selectivity, RET^{V804M} vs KDR
5	(4-benzamide)	0.025 (0.007)	3.7	110	4.4 (0.18)	0.89	2.3
15	Ph	1.14 (0.43)	2.4	0.96			
16	(3-benzamide)	4.3 (1.05)	*n/d*	8.0			
17	(4-sulfonamide)	0.36 (0.14)	1.3	220	> 10	1	1
18	(4-carboxylic acid)	0.56 (0.19)	1.2	1.8			
19	(4-acetamide)	6.7 (1.72)	2.6	4.4			
20	(3-acetamide)	1.6 (0.15)	4.0	22			
21	(4-methanesulfonamide)	1.5 (0.89)	0.28	29			
22	(indazole)	0.30 (0.065)	18	83	2.8 (0.19)	1.9	1.9
23	(benzodioxole)	0.29 (0.16)	0.64	27	1.5 (0.03)	2.2	6.2

[a]All assay values are the geometric mean of at least two independent duplicate determinations, quoted to two significant figures.

Standard deviations are given in parentheses. Biochemical and cellular selectivities are expressed as fold-values.

Similar to many of the derivatives prepared to this point, **23** suffered from modest kinetic solubility (30 µM) and further optimisation was undertaken in an effort to optimise both the cellular activity profile and solubility in parallel. Methods used to synthesise these derivatives are described in Scheme 2. Briefly, formylation of peperacetonitrile with ethyl formate and cyclisation with semicarbazide gave the aminopyrazole **24**, which was further cyclised to **25** and halogenated to give **26**. Finally, S_NAr displacement gave the desired target compounds.
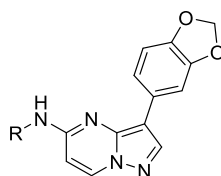
Scheme 2: *Synthesis of compounds 27-35.*
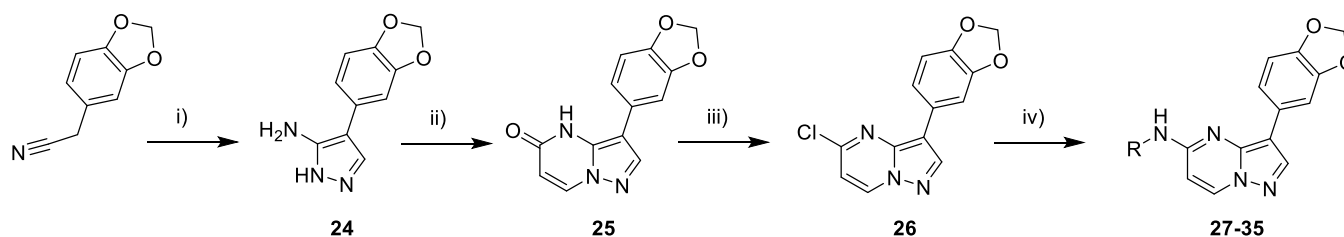
Reagents and conditions: i) a) Ethyl formate, NaOMe, PhMe, reflux, 24h; b) semicarbazide, methanol, 0 °C, 1h; c) NaOH, 100 °C, 30 min, 55% overall; ii) 1,3-dimethyluracil, NaOEt, EtOH, reflux,24h, 83%; iii) POCl₃, DMF, reflux, 1.5h, 78%; iv) amine, DMF, 80 °C, 1h, 11-86%.

In this series of derivatives, alteration of the pyridine regiochemistry improved biochemical potency, but had little effect on cellular activity (compound **27**, Table 3). The importance of both the basic nitrogen and its positioning, were highlighted through the significant loss of potency observed with **28** and **29** respectively, in contrast to the flat SAR observed with **12** and **13**. Saturation of the ring system (compounds **30** and **31**) maintained biochemical potency. Further investigation of these saturated systems led to the open chain amine derivative **34**, which showed a greater than ten-fold increase in cell activity compared to **23**. More importantly, this compound was significantly more selective when assessed in our RET and KDR cell assays, exceeding 25-fold selectivity against both counter-targets for the first time. Whilst more extensive biochemical kinase profiling has not been undertaken on this derivative to fully understand its selectivity profile, the lack of off-target cellular cytotoxicity (4 µM in RET and 9 µM in KDR vs 100 nM in RET[V804M] cell assays) suggests that even this relatively unoptimised derivative is not a promiscuous inhibitor. Compound **34** also showed promising physicochemical properties (kinetic solubility >100 µM; P_{app} 22.8 × 10^{-6} cm/s and efflux ratio 1.4 in a Caco-2 assay) but poor metabolic stability in mouse liver microsomes (MLM CL_{int} = 62 µL/min/mg).

Table 3: Further optimisation of methylenedioxypyrazolopyrimidine compound 23.[a]

Compound	R	RET^{V804M} biochemical IC$_{50}$ (μM)	Biochemical selectivity, RET^{V804M} vs RET	Biochemical selectivity, RET^{V804M} vs KDR	RET^{V804M} cellular IC$_{50}$ (μM)	Cell assay selectivity, RET^{V804M} vs RET	Cell assay selectivity, RET^{V804M} vs KDR
23		0.29 (0.16)	0.64	27	1.5 (0.03)	2.2	6.2
27		0.039 (0.03)	14	100	1.1 (0.03)	3.1	7.6
28		29 (14.6)	0.16	2.3			
29		63 (4.2)	2.1	2.1			
30		0.20 (0.019)	1.2	64	1.3 (0.021)	0.85	2.6
31		0.88 (0.15)	1.2	17			
32		0.091 (0.091)	21	540	0.74 (0.049)	9.8	13
33		0.66 (0.070)	5.3	34			
34		0.019 (0.004)	16	410	0.11 (0.045)	32	76
35		0.13 (0.012)	15	19	6.8 (0.13)	1.5	1.5

[a]All assay values are the geometric mean of at least two independent duplicate determinations, quoted to two significant figures. Standard deviations are given in parentheses. Biochemical and cellular selectivities are expressed as fold-values.

Further confirming target engagement, compounds **13** and **34** were soaked into crystals of the kinase domain of RET^{V804M} (Figure 4b, c). Pleasingly, the crystal structure for **13** accurately recapitulated the binding mode and key interactions predicted by docking, with the benzamide hydrogen-bonding to Lys758, Glu775, the Asp892 backbone

and the pyridine occupying the ribose pocket. However, we were surprised to observe that **34** exhibited a different binding mode, with the pyrazolopyrimidine core adopting a flipped orientation with respect to the hinge, while maintaining a single hinge H-bond to Ala807 backbone amide. The tertiary amine of **34** H-bonds to Asp892 and forms lipophilic contacts with Phe735 and Leu881, while the piperonyl moiety binds somewhat loosely between the walls of the ATP-binding site, bounded by Leu730/Gly731 of the P-loop and Gly810/Ser811 of the ribose pocket, but without making any significant polar interactions. We speculate that the flipping of the binding mode may be a consequence of the binding interactions achieved by the peripheral substituents rather than the bicyclic hinge binder itself. Hence the main driver for the binding orientation of **13** may be the hydrogen-bonding interactions between the benzamide and Lys758/Glu775; these favourable interactions cannot be replicated by the piperonyl moiety of **34**, and thus the flipped binding mode allows for favourable polar and lipophilic interactions from the dimethylamino propyl moiety to Asp892 and neighbouring residues. [We note that both binding orientations for a chemically similar hinge binder can be observed in other kinase X-ray structures on the PDB: for example, 4Z7H, 4YMJ and 3BQR adopt a similar orientation to **13**, while 4TXC and 6AYW bind similarly to **34**.] This alternate binding mode likely also accounts for the differing SAR trends around the pyridylmethyl moiety in the piperonyl series (compounds **23**, **27**), compared to the corresponding benzamide derivatives compounds **5**, **12**).

It is difficult to rationalize fully the improved selectivity of **34** over wild type RET, as there may be many contributing factors arising from the change in substituents and the change in binding mode which would need to be explored by more extensive SAR. The flipped orientation of the hinge binder may result in improved lipophilic contacts with the Met gatekeeper or allow the gatekeeper to adopt a more favoured conformation. The lipophilic amine of **34** is situated in fairly close contact to Ser891 (Figure 4d), and this may contribute to the improved selectivity over KDR (which features a larger Cys sidechain in the equivalent position). Whatever the rationale, it is of interest that the flipped binding orientation has led to diverging SAR for this series.

To our knowledge, this is the first report of RET- and KDR-selective inhibitors of RET^{V804M}, assessed through both biochemical and cellular assays. We believe these compounds may offer useful starting points in the delivery of novel adjunct therapeutics, delivering additional patient benefit alongside the RET inhibitors presently in clinical development.
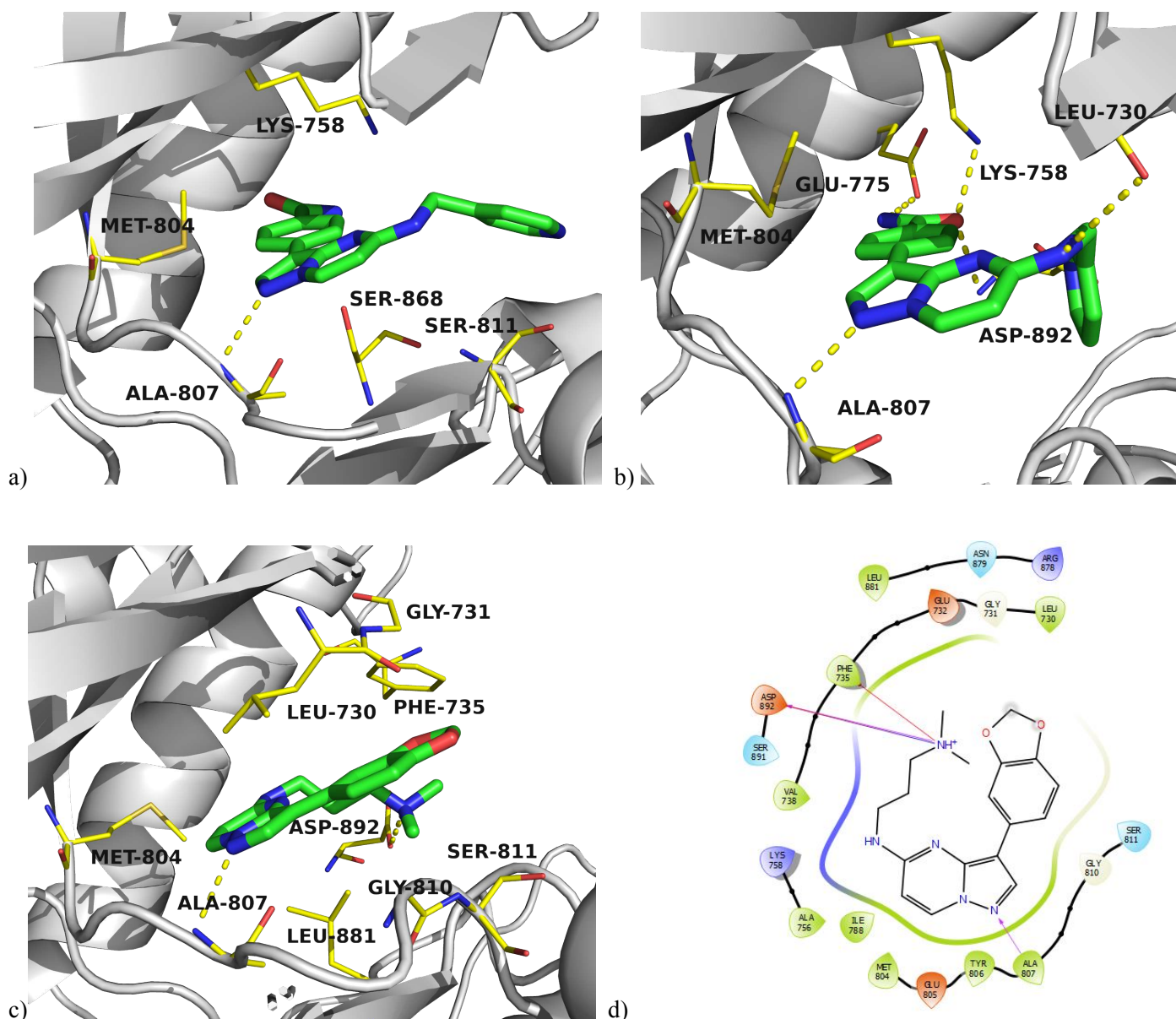
Figure 4: *a) Docked model of early hit **5** bound to RET[V804M]; b) Crystal structure of **13** bound to RET[V804M] (PDB 6I83); c) Crystal structure of optimised lead **34** bound to RET[V804M] (PDB 6I82); d) 2D Ligand interaction plot for **34** bound to RET[V804M]. In all panels, RET[V804M] is shown as grey cartoons, key residues as yellow sticks and the respective ligand as green sticks.*

ASSOCIATED CONTENT.

Supporting Information Assay protocols, purity data for all compounds, general experimental details and representative synthetic procedures. This material is available free of charge at http://pubs.acs.org

Accession Codes

RET[V804M] kinase domain in complex with **13**, 6I83; RET[V804M] kinase domain in complex with **34**, 6I82.

Author information

*Telephone: +44 (0)161 3066272. Email: rebecca.newton@cruk.manchester.ac.uk.

Author contributions.

R.N., B.W. and A.J. wrote the manuscript. R.N., B.W., E.F., N.H., S.J. and A.J. designed and/or synthesised compounds. B.W. conducted the computational aspects of the study. C.S., D.B., M.R., L-Y.L., A.E. and R.B. conducted protein production, crystallography and structure refinement. S.H., H.B., A.W., I.W. and D.O. designed and conducted the biological screening cascade.

Notes

The authors declare no competing financial interests.

ABBREVIATIONS

ALK, anaplastic lymphoma kinase; ATP, adenosine triphosphate; EGFR, epithelial growth factor receptor; HTVS, high-throughput virtual screening; KDR, kinase insert domain; NSCLC, non-small cell lung cancer; RET, re-arranged during transfection; SAR, structure-activity relationship; SP, standard precision virtual screening.

REFERENCES

1.   Kohno, T.; Ichikawa, H.; Totoki, Y.; Yasuda, K.; Hiramoto, M.; Nammo, T.; Sakamoto, H.; Tsuta, K.; Furuta, K.; Shimada, Y.; Iwakawa, R.; Ogiwara, H.; Oike, T.; Enari, M.; Schetter, A. J.; Okayama, H.; Haugen, A.; Skaug, V.; Chiku, S.; Yamanaka, I.; Arai, Y.; Watanabe, S.-i.; Sekine, I.; Ogawa, S.; Harris, C. C.; Tsuda, H.; Yoshida, T.; Yokota, J.; Shibata, T., KIF5B-RET fusions in lung adenocarcinoma. *Nature Medicine* **2012,** *18* (3), 375-377.
2.   Takeuchi, K.; Soda, M.; Togashi, Y.; Suzuki, R.; Sakata, S.; Hatano, S.; Asaka, R.; Hamanaka, W.; Ninomiya, H.; Uehara, H.; Lim Choi, Y.; Satoh, Y.; Okumura, S.; Nakagawa, K.; Mano, H.; Ishikawa, Y., RET, ROS1 and ALK fusions in lung cancer. *Nature Medicine* **2012,** *18* (3), 378-381.
3.   Lipson, D.; Capelletti, M.; Yelensky, R.; Otto, G.; Parker, A.; Jarosz, M.; Curran, J. A.; Balasubramanian, S.; Bloom, T.; Brennan, K. W.; Donahue, A.; Downing, S. R.; Frampton, G. M.; Garcia, L.; Juhn, F.; Mitchell, K. C.; White, E.; White, J.; Zwirko, Z.; Peretz, T.; Nechushtan, H.; Soussan-Gutman, L.; Kim, J.; Sasaki, H.; Kim, H. R.; Park, S.-i.; Ercan, D.; Sheehan, C. E.; Ross, J. S.; Cronin, M. T.; Jänne, P. A.; Stephens, P. J., Identification of new ALK and RET gene fusions from colorectal and lung cancer biopsies. *Nature Medicine* **2012,** *18* (3), 382-384.
4.   Drilon, A.; Wang, L.; Hasanovic, A.; Suehara, Y.; Lipson, D.; Stephens, P.; Ross, J.; Miller, V.; Ginsberg, M.; Zakowski, M. F.; Kris, M. G.; Ladanyi, M.; Rizvi, N., Response to Cabozantinib in patients with RET fusion-positive lung adenocarcinomas. *Cancer Discov* **2013,** *3* (6), 630-5.
5.   Drilon, A.; Rekhtman, N.; Arcila, M.; Wang, L.; Ni, A.; Albano, M.; Van Voorthuysen, M.; Somwar, R.; Smith, R. S.; Montecalvo, J.; Plodkowski, A.; Ginsberg, M. S.; Riely, G. J.; Rudin, C. M.; Ladanyi, M.; Kris, M. G., Cabozantinib in patients with advanced RET-rearranged non-small-cell lung cancer: an open-label, single-centre, phase 2, single-arm trial. *The Lancet. Oncology* **2016,** *17* (12), 1653-1660.
6.   Yoh, K.; Seto, T.; Satouchi, M.; Nishio, M.; Yamamoto, N.; Murakami, H.; Nogami, N.; Matsumoto, S.; Kohno, T.; Tsuta, K.; Tsuchihara, K.; Ishii, G.; Nomura, S.; Sato, A.; Ohtsu, A.; Ohe, Y.; Goto, K., Vandetanib in patients with previously treated RET-rearranged advanced non-small-cell lung cancer (LURET): an open-label, multicentre phase 2 trial. *The Lancet. Respiratory medicine* **2017,** *5* (1), 42-50.
7.   Subbiah, V.; Velcheti, V.; Tuch, B. B.; Ebata, K.; Busaidy, N. L.; Cabanillas, M. E.; Wirth, L. J.; Stock, S.; Smith, S.; Lauriault, V.; Corsi-Travali, S.; Henry, D.; Burkard, M.; Hamor, R.; Bouhana, K.; Winski, S.; Wallace, R. D.; Hartley, D.; Rhodes, S.; Reddy, M.; Brandhuber, B. J.; Andrews, S.; Rothenberg, S. M.; Drilon, A., Selective RET kinase inhibition for patients with RET-altered cancers. *Annals of oncology : official journal of the European Society for Medical Oncology* **2018,** *29* (8), 1869-1876.
8.   Subbiah, V.; Gainor, J. F.; Rahal, R.; Brubaker, J. D.; Kim, J. L.; Maynard, M.; Hu, W.; Cao, Q.; Sheets, M. P.; Wilson, D.; Wilson, K. J.; DiPietro, L.; Fleming, P.; Palmer, M.; Hu, M. I.; Wirth, L.; Brose, M. S.; Ou, S. I.; Taylor, M.; Garralda, E.; Miller, S.; Wolf, B.; Lengauer, C.; Guzi, T.; Evans, E. K., Precision Targeted Therapy with BLU-667 for RET-Driven Cancers. *Cancer Discov* **2018,** *8* (7), 836-849.
9.   Carlomagno, F.; Guida, T.; Anaganti, S.; Vecchio, G.; Fusco, A.; Ryan, A. J.; Billaud, M.; Santoro, M., Disease associated mutations at valine 804 in the RET receptor tyrosine kinase confer resistance to selective kinase inhibitors. *Oncogene* **2004,** *23* (36), 6056-63.
10.   Tan, C. S.; Gilligan, D.; Pacey, S., Treatment approaches for EGFR-inhibitor-resistant patients with non-small-cell lung cancer. *The Lancet. Oncology* **2015,** *16* (9), e447-e459.
11.   Ardini, E.; Banfi, P.; Avanzi, N.; Ciomei, M.; Polucci, P.; Cirla, A.; Anello, M.; Borgia, A. L.; Motto, I.; Cristiani, C.; Ballinari, D.; Felder, E.; Donati, D.; Galvani, A.; Isacchi, A.; Menichincheri, M., Abstract 4785: NMS-E668, a highly potent orally available RET inhibitor with selectivity towards VEGFR2 and demonstrated antitumor efficacy in multiple RET-driven cancer models. *Cancer research* **2018,** *78* (13 Supplement), 4785.
12.   Dagogo-Jack, I.; Stevens, S. E.; Lin, J. J.; Nagy, R.; Ferris, L.; Shaw, A. T.; Gainor, J. F., Emergence of a RET V804M Gatekeeper Mutation During Treatment With Vandetanib in RET-Rearranged NSCLC. *Journal of Thoracic Oncology* **2018,** *13* (11), e226-e227.
13.   eMolecules. https://www.emolecules.com/ (accessed Nov 24, 2018).
14.   Yoon, H.; Kwak, Y.; Choi, S.; Cho, H.; Kim, N. D.; Sim, T., A Pyrazolo[3,4-d]pyrimidin-4-amine Derivative Containing an Isoxazole Moiety Is a Selective and Potent Inhibitor of RET Gatekeeper Mutants. *J Med Chem* **2016,** *59* (1), 358-73.
15.   Dar, A. C.; Das, T. K.; Shokat, K. M.; Cagan, R. L., Chemical genetic discovery of targets and anti-targets for cancer polypharmacology. *Nature* **2012,** *486* (7401), 80-84.
16.   Plenker, D.; Riedel, M.; Brägelmann, J.; Dammert, M. A.; Chauhan, R.; Knowles, P. P.; Lorenz, C.; Keul, M.; Bührmann, M.; Pagel, O.; Tischler, V.; Scheel, A. H.; Schütte, D.; Song, Y.; Stark, J.; Mrugalla, F.; Alber, Y.; Richters, A.; Engel, J.; Leenders, F.; Heuckmann, J. M.; Wolf, J.; Diebold, J.; Pall, G.; Peifer, M.; Aerts, M.; Gevaert, K.; Zahedi, R. P.; Buettner, R.; Shokat, K. M.; McDonald, N. Q.; Kast, S. M.; Gautschi, O.; Thomas, R. K.; Sos, M. L., Drugging the catalytically inactive state of RET kinase in RET-rearranged tumors. *Science translational medicine* **2017,** *9* (394), eaah6144.

Discovery and Optimisation of wt-RET/KDR-selective Inhibitors of RET[V804M] Kinase

Rebecca Newton,[1,*] Bohdan Waszkowycz,[1] Chitra Seewooruthun,[2] Daniel Burschowsky,[2] Mark Richards,[3] Samantha Hitchin,[1] Habiba Begum,[1] Amanda Watson[1], Eleanor French,[1] Niall Hamilton,[1] Stuart Jones,[1] Li-Ying Lin,[4] Ian Waddell,[1] Aude Echalier,[2] Richard Bayliss,[3] Allan M. Jordan[1] and Donald Ogilvie.[1]
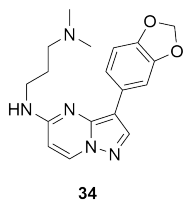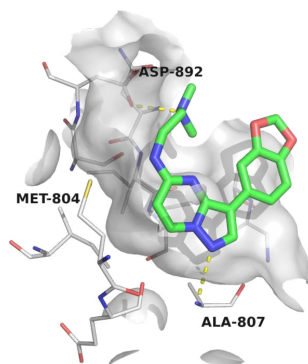
34

RET[V804M] IC$_{50}$	19 nM
Selectivty vs wt-RET	16x
Selectivty vs KDR	410x